M_d = molar flow rate of nitrogen through downstream side of cell
M_u = molar flow rate of nitrogen through upstream side of cell
N_i = flux of species i
N_0 = flux of sulfur dioxide in absence of chemical reactions
N_{H_2O} = flux of sulfur dioxide through water films
Na_{tot} = total alkaline sodium concentration (acid neutralizing capacity)
P_{tot} = total pressure
y_m = mole fraction of sulfur dioxide indicated by Meloy sulfur analyzer
$y_{SO_2,0}$, $y_{SO_2,1}$ = mole fraction sulfur dioxide in gas phase at $x = 0$ and $x = 1$

Subscripts

bl = boundary layer theory (NEBLA)
eq = equilibrium theory

Superscript

$\hat{}$ = dimensional variable or parameter

Greek Letters

γ_i = activity coefficient of species i
δ_0 = boundary layer thickness near $x = 0$
δ_1 = boundary layer thickness near $x = 1$
μ = solution viscosity
Φ = electric field potential

LITERATURE CITED

Bromley, L. A., "Approximate Individual Ion Values of β (or B) in Extended Debye-Huckel Theory for Uni-Univalent Aqueous Solutions at 298.15K," *J. Chem. Thermodynamics*, **4**, 669-73 (1972).

Chilcote, D. D., "The Diffusion of Ions in Agar Gel Suspensions of Red Blood Cells," PhD thesis, Calif. Inst. Technol. (1970).

Davies, C. W., *Ion Association*, Butterworths, Washington, D.C. (1962).

Eigen, M., K. Kustin and G. Maass, "Die Geschwindigkeit der Hydratation von SO_2 in wäBriger Lösung," *Z. Phys. Chem.*, **30**, 130-36 (1961).

Goettler, L. A., "The Simultaneous Absorption of Two Gases in a Reactive Liquid," PhD thesis, Univ. Del., Newark (1967).

Hetherington, P. J., "Absorption of Sulfur Dioxide into Aqueous Media," PhD thesis, Univ. Tasmania, Hobart (1968).

Hikita, H., S. Asai and T. Tsuji, "Absorption of SO_2 into Aqueous Sodium Hydroxide and Sodium Sulphite Solutions," *AIChE J*, **23**, 538-44 (1977).

Hikita, H., S. Asai and H. Nose, "Absorption of Sulfur Dioxide in Water," *ibid.*, **24**, 147-9 (1978).

Johnstone, H. F., and H. C. Blankmeyer, "Recovery of SO_2 from Waste Gases," *Ind. Eng. Chem.*, **30**, 101-9 (1938).

Onda, K., T. Kobayashi, M. Fujine and M. Takahashi, "Behavior of the Reaction Plane Movement in Gas Absorption Accompanied by Instantaneous Chemical Reactions," *Chem. Eng. Sci.*, **26**, 2009-26, 2027-35 (1971).

Phipps, R. L. "The Rate of Hydrolysis of Sulfur Dioxide," B.S. thesis, Mass Inst. Technol., Cambridge (1947).

Roberts, D. L., "Sulfur Dioxide Transport Through Aqueous Solutions," PhD thesis, Calif. Inst. Technol. (1979).

Schultz, J. S., J. D. Goddard and S. R. Suchdeo, "Facilitated Transport via Carrier-Mediated Diffusion in Membranes," *AIChE J*, **20**, 417-45; 625-45 (1974).

Standen, A., ed., *Encyclopedia of Chemical Technology*, 2 ed., Vol. 14, Wiley, New York (1962).

Suchdeo, S. R., and J. S. Schultz, "Mass Transfer of CO_2 Across Membranes," *Biochim. et Biophys. Acta*, **352**, 412-40 (1974).

Takeuchi, H., Y. Maeda and K. Itoh, *Kagaku Kogaku Ronbunshu*, **1**, 252 (1975); quoted by Takeuchi and Yamanaka, *Ind. Eng. Chem. Process Design Develop.*, **17**, 389-93 (1978).

Wang, J. C., and D. M. Himmelblau, "A Kinetic Study of Sulfur Dioxide in Aqueous Solution with Radioactive Tracer," *AIChE J*, **10**, 574-80 (1964).

Weast, R. C., *Handbook of Chemistry and Physics*, 52 ed., Chemical Rubber Company, Cleveland, Ohio (1971).

Manuscript received March 12, 1979; revision received January 17, and accepted January 23, 1980.

Aerosol Behavior in The Continuous Stirred Tank Reactor

JAMES G. CRUMP

and

JOHN H. SEINFELD

Department of Chemical Engineering
California Institute of Technology
Pasadena, California 91125

The basic features of aerosol behavior in the CSTR are examined. Solutions are obtained for the steady state aerosol size distribution during simultaneous coagulation, particle growth by vapor condensation and new particle formation by nucleation. Explicit distributions are shown for the case of a monodisperse feed aerosol.

SCOPE

Studies of particle formation and evolution in combustion systems and in laboratory simulations of atmospheric chemistry sometimes involve the use of a CSTR. The interpretation of aerosol size distributions in a CSTR requires the development and solution of the general population balance equation applicable to that system. The phenomena that must be considered include coagulation, particle growth by vapor condensation and new particle formation by vapor nucleation. Because the general problem of aerosol behavior in the CSTR does not appear to have been studied previously, an examination of the qualitative features of the steady state size distributions that may be achieved is deemed an appropriate first step to a more in depth analysis. Of particular interest is the elucidation of the effects of varying residence time and the characteristic times for coagulation and growth by condensation on the size distributions attained.

0001-1541-80-3904-0610-$00.75.

CONCLUSIONS AND SIGNIFICANCE

A general solution for the steady state aerosol size distribution in a CSTR is obtained for an arbitrary feed aerosol size distribution and for kinetic coagulation coefficient and particle growth rate that are independent of particle size. The object of the analysis is to demonstrate the qualitative features of the size distribution, and, consequently, the simplified functional forms of the coagulation and growth coefficients were chosen so as to enable exact solution of the governing equations. The solution is explicitly illustrated for a monodisperse feed aerosol. Although the assumption of a constant coagulation coefficient is valid in certain instances, that of a size independent growth rate is not. Thus, the case of growth rate linearly proportional to particle volume is investigated as a perturbation to the constant growth case to determine the qualitative effect of the size dependent growth rate. Although simulation of a specific system will generally require numerical solution of the aerosol balance equation employing the proper detailed expressions for the coagulation and growth coefficients, the solutions presented here provide an indication of the expected behavior of the size distribution as residence time and other physical parameters are varied. In addition, the dimensionless groups governing aerosol behavior in a CSTR are defined. The groups indicate that for any system of this type, the relative magnitudes of the characteristic times for growth, coagulation and reactor residence will strongly influence the expected size distribution.

Understanding the processes associated with particle formation and evolution in combustion systems and in laboratory simulations of atmospheric chemistry requires consideration of aerosol behavior in typical chemical reactor configurations, particularly the continuous stirred tank reactor (CSTR) and the tubular flow reactor. The object of this work is to elucidate the basic features of aerosol behavior in the CSTR.

A variety of physical and chemical phenomena influence the size distribution of aerosols, including coagulation, growth by condensation of gases on the particles and formation of fresh particles by nucleation. In this work, we consider a general situation in which an aerosol of known size distribution is introduced into a CSTR together with a vapor species capable of transferring to the aerosol by condensation or of nucleating to form new particles. Thus, simultaneous coagulation, growth and new particle formation may occur in the reactor.

The equations governing the steady state aerosol size distribution and vapor concentration are presented and nondimensionalized. A general solution of these equations is then obtained for the case in which the kinetic coefficient of coagulation is independent of the sizes of the two particles and in which the rate of growth of an individual particle by condensation is independent of the size of the particle. The solution is explicitly illustrated for a monodisperse feed aerosol. Although the assumption of a constant coagulation coefficient is valid in certain instances, that of a size independent growth rate is generally not. Thus, the case of growth rate linearly proportional to particle volume and a monodisperse feed aerosol is then investigated to determine the effect of size dependent growth rate on the steady state aerosol size distribution.

EQUATIONS DESCRIBING GAS-AEROSOL BEHAVIOR IN A CSTR

Consider a CSTR operated at steady state in which an aerosol of known size distribution is fed into the reactor together with a gas, which condenses on the aerosol. The aerosol is characterized by its size distribution function $n(v)$, where $n(v)dv$ represents the number density of particles having volumes between v and $v + dv$. The molar concentration of the gas is denoted by c. Gas at concentration c_0 is continuously introduced into the reactor at volume flow rate q together with an aerosol of size distribution $n_0(v)$. The gas-aerosol system undergoes the following processes: condensation of the gas on the aerosol particles, homogeneous nucleation of the gas to produce new particles of a given volume v_0 and coagulation or coalescence of aerosol particles to form larger particles.

Let $S_0(c)$ be the rate of formation of particles by nucleation and $I(v) = cf(v)$ be the growth rate of a particle of volume v by condensation. The form $cf(v)$ assumes that condensation is irreversible, a good assumption for low vapor pressure gaseous species. Conservation of mass for aerosol and gas gives

$$q(c_0 - c) = 10^{-12}\left(\frac{\rho}{M}\right) Vc \int_0^\infty f(v)n(v)dv + 10^{-12}\left(\frac{\rho}{M}\right) Vv_0S_0(c) \quad (1)$$

$$q[n_0(v) - n(v)] + VS_0(c)\delta(v - v_0) - Vc\frac{d}{dv}[f(v)n(v)] + \frac{V}{2}\int_0^v \beta(v - \tilde{v}, \tilde{v})n(v - \tilde{v})n(\tilde{v})d\tilde{v} - Vn(v)\int_0^\infty \beta(v, \tilde{v})n(\tilde{v})d\tilde{v} = 0 \quad (2)$$

We note that the factors of 10^{-12} appear because particle volume is expressed in μm^3, whereas density has units of g cm^{-3}. It has been assumed that the total aerosol volume is small compared to that of the gas, so that the total volumetric flow rate for the mixture of gas and aerosol may be replaced by that of the gas alone, q. Unless the density of aerosol particles is extremely high, the right-hand side of Equation (1) will be negligible, and the gas concentration c will be the same as the feed gas concentration c_0. In any case, we will henceforth suppose that c is known and deal only with the aerosol balance, Equation (2). The boundary condition on (2) is

$$n(0) = 0 \quad (3)$$

All realistic distributions will also satisfy the condition $n(v) = 0$ as $v \to \infty$.

Because of the complex dependence of the coagulation coefficient $\beta(v, \tilde{v})$ and the condensation function $f(v)$ on the particle volume v, (2) must generally be solved numerically. In the present study, however, we are interested in elucidating the qualitative features of the solutions to (2) and for this reason will consider constant coagulation coefficient $\beta(v, \tilde{v}) = \beta$ and size independent condensation rate $f(v) = \sigma_v$. The validity of these assumptions has been discussed elsewhere (Ramabhadran et al., 1976). We note, in particular, that the assumption of constant β is physically realistic in the initial stages of Brownian coagulation of a monodisperse aerosol. However, the assumption of size independent growth is not in general obeyed. Usually, $f(v)$ can be expressed as $f(v) = \sigma_\gamma v^\gamma$, $0 \le \gamma \le 1$ (Ramabhadran et al., 1976).

With the above assumptions, (2) becomes

$$Vc\sigma_0 n'(v) = \frac{1}{2} V\beta n^*(v) - V\beta n(v)\int_0^\infty n(\tilde{v})d\tilde{v} + q[n_0(v) - n(v)] + VS_0\delta(v - v_0) \quad (4)$$

where

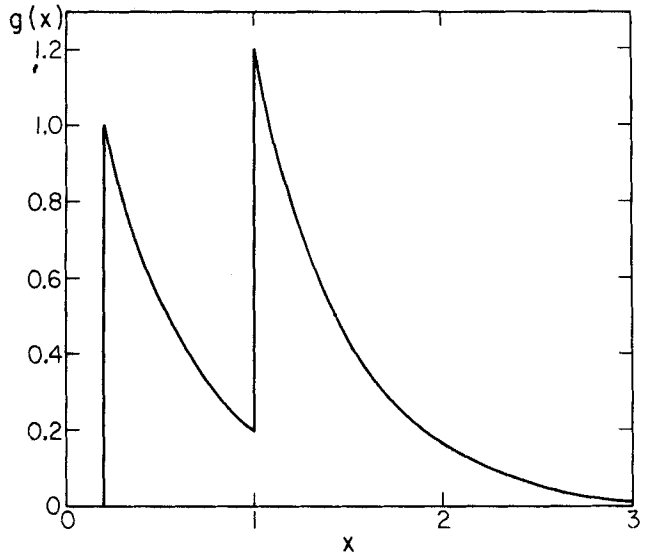

Figure 1. Dimensionless size distribution g(x) for monodisperse feed and no coagulation: $\kappa = 0$, $\alpha = 0.5$, $\omega = 0.5$, $x_0 = 0.2$.

$$n*n(v) \equiv \int_0^v n(v - \tilde{v})n(\tilde{v})\, d\tilde{v}$$

and $S_0 \equiv S_0(c)$.

We introduce the total number and volume densities of the aerosol

$$N = \int_0^\infty n(v)\, dv \qquad N_0 = \int_0^\infty n_0(v)\, dv$$

$$\bar{V} = \int_0^\infty vn(v)\, dv \qquad \bar{V}_0 = \int_0^\infty vn_0(v)\, dv$$

and the following dimensionless groups, $\alpha = \theta c\sigma_0 N_0/\bar{V}_0$, $\kappa = \beta\theta N$, $\omega = \theta S_0/N$, where the mean residence time $\theta = V/q$. α, κ and ω are ratios of residence time to characteristic condensation, coagulation and nucleation times, respectively.

Dimensionless particle volume and aerosol size distribution are defined as

$$x = N_0 v/\bar{V}_0$$

$$g(x) = \frac{\bar{V}_0}{N_0 N}\, n\left(\frac{\bar{V}_0 x}{N_0}\right)$$

Then, (4) becomes

$$\alpha g'(x) = \frac{1}{2}\kappa g*g(x) - (1 + \kappa)g(x) + g_0(x) + \omega\delta(x - x_0) \quad (5)$$

Note that the feed distribution $g_0(x)$ and the nucleation term $\omega\delta(x - x_0)$ play equivalent roles in (5); so, for simplicity, we combine them, setting $g_1(x) = g_0(x) + \omega\delta(x - x_0)$.

It is necessary to evaluate the steady state number density N. By integration of (4) from 0 to ∞ and solution of the resulting quadratic equation for N, one obtains

$$N = \frac{1}{\beta\theta}\left[\sqrt{1 + 2\beta\theta(N_0 + \theta S_0)} - 1\right] \quad (6)$$

Subsequently we shall be interested in a monodisperse feed distribution $n_0(v) = N_0\delta(v - v_f)$. Using (6), we find that

$$g_0(x) = \left(1 + \frac{1}{2}\kappa - \omega\right)\delta(x - 1) \quad (7)$$

STEADY STATE SOLUTIONS

In this section we examine solutions of the material balance (5). First we consider special cases in which one or more of the physical processes is unimportant.

No Coagulation; $\kappa = 0$

In the absence of coagulation, the aerosol fed to the reactor grows by condensation, and fresh aerosol forms by nucleation. There is no particle-particle interaction. Equation (5) can be easily solved to yield

$$g(x) = \frac{1}{\alpha}\left\{\int_0^x e^{-y/\alpha} g_0(x - y)\, dy + \omega U(x - x_0)e^{-(x-x_0)/\alpha}\right\} \quad (8)$$

where U is the unit step function

$$U(x) = \begin{cases} 0 & x \le 0 \\ 1 & x > 0 \end{cases}$$

For a monodisperse feed, g_0 is given by (7), and

$$g(x) = \frac{1}{\alpha}\{(1 - \omega)U(x - 1)e^{-(x-1)/\alpha} + \omega U(x - x_0)e^{-(x-x_0)/\alpha}\} \quad (9)$$

Figure 1 shows $g(x)$ for $0 < x_0 < 1$. Physically, we note that the size distribution $g(x)$ exhibits two peaks corresponding to the sizes of the feed aerosol ($x = 1$) and that freshly formed by nucleation ($x = x_0$). The distribution spreads toward larger sizes because of the condensation growth. The peak at $x = 1$ is higher than it would be in the absence of nucleation because some of the smaller particles have grown by condensation to sizes ≥ 1 and augment the feed aerosol. The degree of spreading of the distribution is controlled by the dimensionless parameter α, which depends upon the residence time θ.

No Nucleation; $\omega = 0$

When nucleation may be neglected, (5) becomes

$$\alpha g'(x) = \frac{1}{2}\kappa g*g(x) - (1 + \kappa)g(x) + g_0(x) \quad (10)$$

Equation (10) can be solved by Laplace transformation (see appendix) to yield the general solution for the aerosol size distribution

$$g(x) = \sum_{k=0}^{\infty} \frac{\kappa^k[\phi_k^* g_0^{*(k+1)}]\,(x)}{2^k k!(k + 1)!\alpha^{2k+1}} \quad (11)$$

where

$$\phi_k(x) = x^{2k}e^{-(1+\kappa)x/\alpha} \quad (12)$$

and g_0^{*k} denotes the k fold convolution of g_0 defined by

$$g_0^{*k}(x) = g_0^* g_0^* \ldots *g_0(x)$$

Again, if the aerosol in the feed is monodisperse, so that $g_0(x) = (1 + 1/2\kappa)\delta(x - 1)$, then

$$g_0^{*(k+1)}(x) = \left(1 + \frac{1}{2}\kappa\right)^{k+1}\delta[x - (k + 1)] \quad (13)$$

and

$$\phi_k^* g_0^{*(k+1)} = \left(1 + \frac{1}{2}\kappa\right)^{k+1}[x - (k + 1)]^{2k} \times U[x - (k + 1)]e^{-(1+\kappa)[x-(k+1)]/\alpha} \quad (14)$$

The resulting distribution is thus

$$g(x) = \sum_{k=0}^{\infty} \frac{\kappa^k(1 + 1/2\kappa)^{k+1}[x - (k + 1)]^{2k}U[x - (k + 1)]e^{-(1+\kappa)[x-(k+1)]/\alpha}}{2^k k!(k + 1)!\alpha^{2k+1}} \quad (15)$$

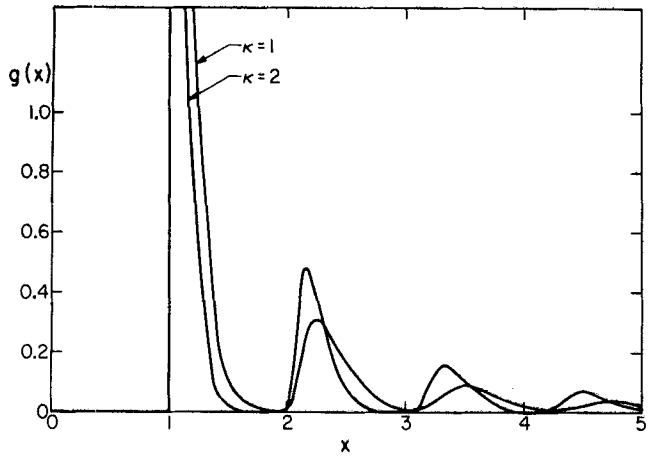

Figure 2. Dimensionless size distribution g(x) for monodisperse feed and no nucleation: $\kappa = 1$ and 2, $\alpha = 0.25$, $\omega = 0$.

To observe the physical significance of this solution, let us examine the case in which $\alpha << 1$, that is, when the characteristic time for condensation is large relative to the residence time. For small α, the function

$$U[x - (k+1)]\,[x - (k+1)]^{2k} e^{-(1+\kappa)[x-(k+1)]/\alpha} / \alpha^{2k+1}$$

which appears in the k^{th} term of the series for $g(x)$ is sharply peaked near $x = k + 1$. The area beneath the peak is $(2k)!/(1+\kappa)^{2k+1}$, so that the above function behaves like $(2k)!\delta[x - (k+1)]/(1+\kappa)^{2k+1}$. It then follows that the distribution behaves like the solution of (5) when $\alpha = \omega = 0$:

$$g(x) = \sum_{k=0}^{\infty} \frac{\kappa^k (1 + 1/2\kappa)^{k+1} \delta[x - (k+1)]\,(2k)!}{2^k (k+1)!k!(1+\kappa)^{2k+1}} \qquad (16)$$

In fact, this solution consists simply of a series of spikes at $x = 1, 2, 3, \ldots$. Physically, this is plausible because coagulation is the only process by which the distribution evolves. Since the dimensionless feed distribution consists only of particles of size $x = 1$, only integer multiples of this size will result. If α is nonzero but still small, roughly the same distribution will be obtained, that is, peaked at the positive integers, but with some spreading toward larger sizes due to condensation. If α is sufficiently small, the peaks will be sharp and will not significantly overlap. Consequently, the distribution can be constructed by taking each term in the series individually. Thus, the peaks occur at approximately $x = (k+1) + 2k\alpha/(1+\kappa)$, $k = 0, 1, 2, \ldots$. The increased shift of the peaks at larger particle sizes results because, on the average, the larger particles have remained in the reactor longer and thus have had a longer time during which to grow. Figure 2 shows the distributions corresponding to $\alpha = 0.25$, and $\kappa = 1$ and 2.

General Solution

Now consider the case in which all processes occur. The general solution of (5) is given by (11), with g_0 replaced by $g_1 = g_0 + \omega\delta(x - x_0)$:

$$g(x) = \sum_{k=0}^{\infty} \frac{\kappa^k \{\phi_k^*[g_0 + \omega\delta(x - x_0)]\}^{*(k+1)}(x)}{2^k k!(k+1)!\alpha^{2k+1}} \qquad (17)$$

Once again, consider the monodisperse feed distribution (7), in which case the size distribution in the CSTR is

$$g(x) = \sum_{k=0}^{\infty} \frac{\kappa^k}{2^k k!(k+1)!\alpha^{2k+1}} \sum_{j=0}^{k+1} \binom{k+1}{j} \times \left(1 + \frac{1}{2}\kappa - \omega\right)^j \omega^{k+1-j} \times U\{x - [j + (k+1-j)x_0]\} \times \{x - [j + (k+1-j)x_0]\}^{2k} e^{-\frac{(1+\kappa)}{\alpha}\{x-[j+(k+1-j)x_0]\}} \qquad (18)$$

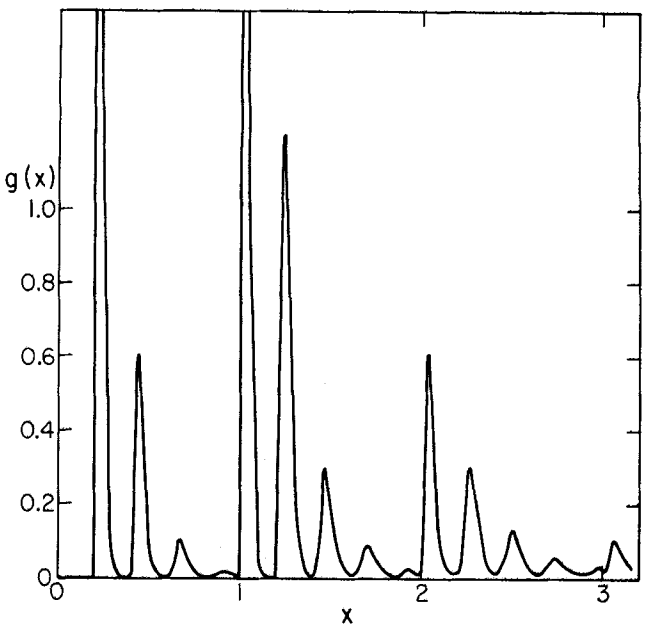

Figure 3. Dimensionless size distribution g(x) for monodisperse feed, including effects of coagulation, condensation and nucleation: $\kappa = 2$, $\alpha = 0.05$, $\omega = 1$, $x_0 = 0.2$.

As before, for small α (small condensation rate), the distribution approaches a sequence of delta functions

$$g(x) = \sum_{j=0}^{\infty} \sum_{k=j-1}^{\infty} \frac{\kappa^k (2k)!}{2^k k!(k+1)!(1+\kappa)^{2k+1}} \times \binom{k+1}{j} \left(1 + \frac{1}{2}\kappa - \omega\right)^j \omega^{k+1-j} \delta\{x - [j + (k+1-j)x_0]\} \qquad (19)$$

The peaks in the distribution (19) occur at all points $j + (k+1-j)x_0$, $k = 0, 1, 2, \ldots$, $j = 0, 1, 2, \ldots, k+1$. These points correspond to all possible sizes that can be formed by coagulation of particles initially of sizes 1 and x_0. For each value of k, the peaks at $j + (k+1-j)x_0$ represent the possible ways in which $k+1$ particles in a mixture of sizes 1 and x_0 may combine.

If $\alpha \neq 0$, the peaks are spread somewhat and shifted owing to condensation. Under the assumption that α is small enough so that the peaks do not overlap substantially, the peak at $x = j + (k+1-j)x_0$ is shifted to the right by $2k\alpha/(1+\kappa)$.

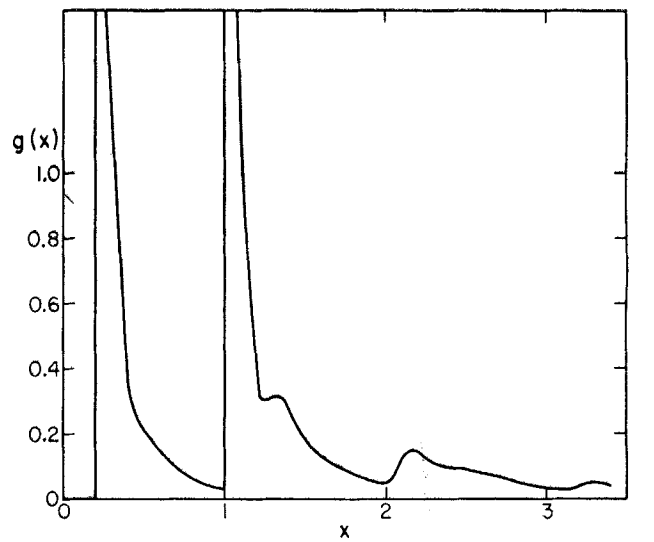

Figure 4. Dimensionless size distribution g(x) for monodisperse feed, including effects of coagulation, condensation and nucleation: $\kappa = 2$, $\alpha = 0.25$, $\omega = 1$, $x_0 = 0.2$.

It is interesting to note that for each k, the $k+1$ peaks at $j+(k+1-j)x_0$ for $j=0,1,\ldots,k+1$ are distributed binominally. This is precisely the distribution one would expect from random combination of particles of sizes 1 and x_0 originally in the ratio $N_0/\theta S_0 = (1 + 1/2\ \kappa-\omega)/\omega$. This phenomenon is illustrated in Figure 3, in which $N_0/\theta S_0=1$, and the peaks at 0.4, 1.2 and 2.0, corresponding to the three possible two-particle combinations, have the magnitude ratios 1:2:1. Similarly, the peaks near 0.7, 1.5, 2.3 and 3, corresponding to all three-particle combinations, have the ratios 1:3:3:1.

As α increases, eventually the peaks overlap, as shown in Figure 4. Only the peaks at x_0 and 1 retain their distinctiveness.

ANALYSIS FOR SIZE DEPENDENT GROWTH RATE

In the previous section, it was assumed that the condensation growth rate of a particle was independent of its size; that is, $I(v) = \sigma_0 c$. Although this assumption enabled us to elucidate the general features of the CSTR size distribution, particle growth rates are, in general, a function of particle size. For a monodisperse feed distribution we have seen that the effect of condensation with a size independent growth rate is to spread and shift to the right the peaks in the size distribution resulting from coagulation. The greater spreading of the distribution at larger sizes was seen to be due to the longer residence time of the larger particles. With a size dependent growth rate of the form $I(v) = c\sigma_\gamma v^\gamma$, $0 < \gamma \leq 1$, we expect an even greater spreading of the distribution at larger sizes, but without a qualitative change in the nature of the distribution. In this section we consider the growth rate $I(v) = c\sigma_1 v$, which represents the maximum growth rate possible. The physical basis for such a growth rate has been discussed by Gelbard and Seinfeld (1979). In short, one obtains this expression when particle growth is chemical reaction controlled.

The aerosol material balance is

$$c\sigma_1 v n'(v) + c\sigma_1 n(v) = \frac{1}{2}\beta n^* n(v) - \beta n(v)\int_0^\infty n(\tilde{v})d\tilde{v} + \frac{1}{\theta}[n_0(v) - n(v)] \quad (20$$

where we have now dropped the nucleation term because of the equivalence of feed and nucleation sources demonstrated previously.

The equation is nondimensionalized as before with the exception that the condensation parameter α is now defined as

$$\alpha = \theta c \sigma_1$$

In dimensionless form, (20) is

$$\alpha x g'(x) + \alpha g(x) = \frac{1}{2}\kappa g^* g(x) - (1 + \kappa)g(x) + g_0(x) \quad (21)$$

Equation (21) is not amenable to solution by Laplace transformation. Therefore we will explore the behavior of g for small α. The important qualitative features of the solution will emerge in this case. We consider the monodisperse feed distribution $g_0(x) = (1 + 1/2\ \kappa)\delta(x-1)$.

When $\alpha=0$, the solution is, as we know, entirely discrete. For small $\alpha>0$, there will be some spreading introduced into the distribution, the spreading increasing with particle size. Because of the fundamental change in the character of the solutions from $\alpha=0$ to $\alpha\neq0$, the analysis of the case of small α leads to a singular perturbation problem. This behavior is also reflected in the fact that the perturbing term $\alpha x g'(x)$ is not small when x is near a natural number, since there $g'(x)$ is very large.

Since nonzero values of g are expected to occur in small regions about each natural number k, we replace the term $\alpha x g'(x)$ in (21) by $\alpha k g'(x)$ for x near k. To begin, let us obtain an expression for the size distribution of the first peak, $x=1$. Let $\psi_1(x)$ represent this function. Note that no particles which have undergone coagulation will be in the size range of the first peak. Consequently, to obtain ψ_1, we may drop the term $1/2\ g^*g(x)$ in (21). The term $xg'(x)$ is replaced by $g'(x)$ since $x=1$, and we drop the term $\alpha g(x)$ since it is negligible compared to $(1+\kappa)g(x)$. Hence, ψ_1 is governed by

$$\alpha\psi_1'(x) = -(1+\kappa)\psi_1(x) + (1 + \frac{1}{2}\kappa)\delta(x-1) \quad (22)$$

Equation (22) may be solved to yield

$$\psi_1(x) = \frac{\left(1+\frac{1}{2}\kappa\right)}{\alpha} e^{-\frac{(1+\kappa)}{\alpha}(x-1)} U(x-1) \quad (23)$$

The function ψ_1 of (23), describing a sharp peak at $x=1$, is, in fact, identical to the first term in the series (15). This is physically plausible, since near $x=1$ the constant and linear growth terms are nearly the same.

If, however, we choose not to replace $xg'(x)$ by $g'(x)$, the equation governing ψ_1 is

$$\alpha x\psi_1'(x) = -(1+\kappa)\psi_1(x) + \left(1 + \frac{1}{2}\kappa\right)\delta(x-1) \quad (24)$$

the solution of which is

$$\psi_1(x) = \frac{\left(1 + \frac{1}{2}\kappa\right)}{\alpha} x^{-\frac{(1+\kappa)}{\alpha}} U(x-1) \quad (25)$$

The function in (23) is, however, an asymptotic approximation to this function, for if $0 \leq x-1 \geq \sqrt{\epsilon}$, then $x^{-1/\epsilon} \sim e^{-(x-1)/\epsilon}$ as $\epsilon \to 0^+$. Outside this asymptotic region, both functions are essentially zero. For the sake of simplicity, however, (23) is the preferred expression, so we shall employ it in subsequent calculations.

We now turn to the calculation of ψ_2, which is the distribution near the peak at $x=2$. We set $x=2$ in the coefficient of the first term, in (21). Now we must retain the coagulation term, because coagulation is the principal mode by which particles of size $x \cong 2$ are formed. Nevertheless, this term can be simplified since the full term $1/2\ \kappa(\psi_1+\psi_2)^*(\psi_1+\psi_2)$ may be approximated by $1/2\kappa\psi_1^*\psi_1$ near $x=2$. Hence, the governing equation for ψ_2 is

$$2\alpha\psi_2'(x) = \frac{1}{2}\kappa\psi_1^*\psi_1(x) - (1+\kappa)\psi_2(x) \quad (26)$$

the solution of which is

$$\psi_2(x) = U(x-2)\left\{\frac{\kappa\left(1 + \frac{1}{2}\kappa\right)^2}{\alpha(1+\kappa)^2} e^{-\frac{(1+\kappa)}{2\alpha}(x-2)} - \frac{\kappa\left(1 + \frac{1}{2}\kappa\right)^2}{\alpha(1+\kappa)^2} e^{-\frac{(1+\kappa)}{\alpha}(x-2)} - \frac{\kappa\left(1 + \frac{1}{2}\kappa\right)^2}{2\alpha^2(1+\kappa)}(x-2)e^{-\frac{(1+\kappa)}{\alpha}(x-2)}\right\} \quad (27)$$

The calculation of ψ_3 and subsequent functions proceeds in an analogous manner. In the case of ψ_3, the coagulation term contains only the convolution products of ψ_1 and ψ_2, since only these contribute significantly to the peak near $x=3$. The equation for ψ_3 is

$$3\alpha\psi_3'(x) = \kappa\psi_1^*\psi_2(x) - (1+\kappa)\psi_3(x) \quad (28)$$

the solution of which is

$$\psi_3(x) = U(x-3)\left\{\frac{27\kappa^2\left(1+\frac{1}{2}\kappa\right)^3}{16\alpha(1+\kappa)^4} e^{-\frac{(1+\kappa)}{3\alpha}(x-3)}\right.$$

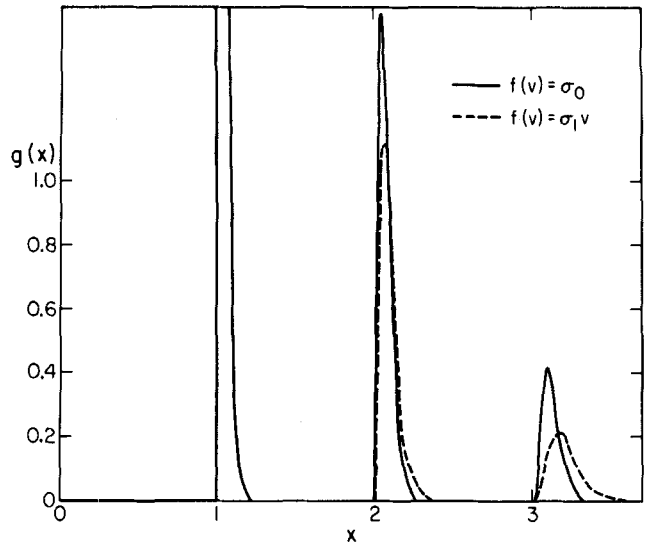

Figure 5. Comparison of dimensionless size distributions resulting from constant and linear condensation rates, $f(v) = \sigma_0$ and $f(v) = \sigma_1 v$, respectively, and monodisperse feed: $\kappa = 1$, $\alpha = 0.05$ in both cases.

$$+\frac{37\kappa^2\left(1+\frac{1}{2}\kappa\right)^3}{16\alpha(1+\kappa)^4}e^{-\frac{(1+\kappa)}{\alpha}(x-3)}-\frac{4\kappa^2\left(1+\frac{1}{2}\kappa\right)^3}{\alpha(1+\kappa)^4}e^{-\frac{(1+\kappa)}{2\alpha}(x-3)}$$

$$+\frac{7\kappa^2\left(1+\frac{1}{2}\kappa\right)^3}{8\alpha^2(1+\kappa)^3}(x-3)\,e^{-\frac{(1+\kappa)}{\alpha}(x-3)}$$

$$+\frac{\kappa^2\left(1+\frac{1}{2}\kappa\right)^3}{8\alpha^3(1+\kappa)^2}(x-3)^2e^{-\frac{(1+\kappa)}{\alpha}(x-3)}\Bigg\} \qquad (29)$$

The sum $\psi_1 + \psi_2 + \psi_3$ represents the solution to (21) for the first three peaks in the distribution. The only limitation in this analysis is that the peaks must be sharp and the distributions about each peak must not overlap. As i increases, the peaks of the ψ_i tend to broaden, so that at a certain point this approach is no longer valid. Nevertheless, the first few peaks in the distribution provide an indication of the differences between the cases of size independent and size dependent particle growth rates. Figure 5 shows the distributions in these two cases. We see, as expected, that the effect of a linear size dependent growth rate is an acceleration of the broadening and a shift to the right of the peaks.

CONCLUSIONS

The qualitative features of aerosol formation and growth in a CSTR have been studied. Exact analytical solutions have been obtained to the aerosol balance equation in the case in which the kinetic coagulation coefficient and the particle growth rate by vapor condensation are independent of particle size. A perturbation solution has also been obtained for the case of linear volume dependent particle growth and a monodisperse feed aerosol.

The assumptions required to obtain these solutions are simplified, but they may nevertheless be useful in understanding the qualitative features of real systems, and in the case in which the feed is monodisperse and Brownian coagulation is occurring in the reactor, these solutions may, in fact, be reasonable approximations to the actual size distributions.

In addition, the important dimensionless groups governing aerosol behavior in a CSTR have been elucidated. These groups are ratios of characteristic times for coagulation, condensation and nucleation to the mean residence time and can be expected to play an important role in aerosol systems even when the simplifying assumptions employed here do not apply.

ACKNOWLEDGMENT

This work was supported by National Science Foundation grant PFR 76-04179.

APPENDIX: SOLUTION OF EQUATION (10)

The aerosol balance equation is

$$\alpha g'(x) = \frac{1}{2}\kappa g^* g(x) - (1+\kappa)g(x) + g_0(x) \qquad (A1)$$

Application of the Laplace transform to (A1) gives

$$\alpha s G(s) = \frac{1}{2}\kappa G^2(s) - (1+\kappa)G(s) + G_0(s) \qquad (A2)$$

where

$$G(s) \equiv \int_0^\infty e^{-sx} g(x)\,dx$$

Equation (A2) may be readily solved for $G(s)$, and we obtain

$$G(s) = (\xi - \sqrt{\xi^2 - 2\kappa G_0(s)})/\kappa \qquad (A3)$$

where $\xi = (\alpha s + 1 + \kappa)$. Taylor expansion of $G(s)$ in powers of $G_0(s)$ gives

$$G(s) = \frac{G_0(s)}{\xi} + \sum_{k=0}^{\infty} \frac{(2k+1)!}{2^k k!(k+2)!}\frac{\kappa^{k+1}}{\xi^{2k+3}} G_0^{k+2}(s) \qquad (A4)$$

If we denote by ϕ the function defined by

$$\phi_k(x) \equiv x^{2k} e^{-\frac{(1+\kappa)}{\alpha}x} \qquad (A5)$$

then we see that

$$\phi_k = (2k)!\,\phi_0^{*(2k+1)} \qquad (A6)$$

where

$$\phi_0(x) \equiv e^{-\frac{(1+\kappa)}{\alpha}x} \qquad (A7)$$

and ϕ_0^{*k} denotes the k fold convolution of ϕ_0. Since under the Laplace transform, $\phi_0 \to \alpha/\xi$, we see that

$$\phi_0^{*(2k+3)} \to \frac{\alpha^{2k+3}}{\xi^{2k+3}}$$

or, equivalently, that

$$\frac{\phi_{k+1}}{(2k+2)!\alpha^{2k+3}} \to \frac{1}{\xi^{2k+3}}$$

Thus, termwise inversion of (A4) gives

$$g(x) = \frac{1}{\alpha}(g_0 * \phi_0)(x) + \sum_{k=1}^{\infty} \frac{\kappa^k[\phi_k^* g_0^{*(k+1)}](x)}{2^k k!(k+1)!\alpha^{2k+1}}$$

$$= \sum_{k=0}^{\infty} \frac{\kappa^k[\phi_k^* g_0^{*(k+1)}](x)}{2^k k!(k+1)!\alpha^{2k+1}} \qquad (A8)$$

NOTATION

c	= vapor concentration, g-mole cm^{-3}
c_0	= vapor concentration in feed, g-mole cm^{-3}
$f(v)$	= volume function appearing in I(v), $\sigma_\gamma v^\gamma$, $\mu m^3 s^{-1}$ (g-mole cm^{-3})$^{-1}$
$g(x)$	= dimensionless size distribution function

$I(v)$ = rate of change of the volume of a particle by vapor condensation, $\mu m^3 s^{-1}$
M = molecular weight of the gas, g mole^{-1}
$n(v)$ = size distribution function μm^{-3} cm^{-3}
$n_0(v)$ = size distribution function of feed aerosol, μm^{-3} cm^{-3}
N = total aerosol number concentration, cm^{-3}
N_0 = total aerosol number concentration in feed, cm^{-3}
q = volumetric flow rate through CSTR, cm^{3}s^{-1}
S_0 = rate of formation of particles by nucleation, cm^{-3} s^{-1}
$U(x)$ = unit step function
v = particle volume, μm^3
v_f = volume of feed aerosol, μm^3
v_0 = volume of particles formed by nucleation, μm^3
V = CSTR volume, cm^3
$\bar{V}$ = total aerosol volume concentration, $\mu m^3 cm^{-3}$
$\bar{V}_0$ = total aerosol volume concentration in feed, $\mu m^3 cm^{-3}$
x = dimensionless particle volume, $N_0 v/\bar{V}_0$
x_0 = $N_0 v_0/\bar{V}_0$

Greek Letters

α = $\theta c_0 \sigma_0 N_0/\bar{V}_0$ or $\theta c_0 \sigma_1$
$\beta(v,\tilde{v})$ = coagulation coefficient, cm^{3}s^{-1}
γ = exponent in growth rate expression
$\delta(v)$ = Dirac delta function
$\delta(x)$ = $\bar{V}_0 \delta(v)/N_0$
θ = V/q
κ = $\beta\theta N$
ρ = liquid density of aerosol particles, g cm^{-3}
σ_γ = constant in expression for $f(v)$, $\mu m^{3-3\gamma}$ s^{-1}(g-mole cm^{-3})$^{-1}$
$\psi_i(x)$ = size distribution around i^{th} peak in the size distribution
ω = $\theta S_0/N$
$*$ = convolution operator

LITERATURE CITED

Gelbard, F., and J. H. Seinfeld, "Exact Solution of the General Dynamic Equation for Aerosol Growth by Condensation," *J. Colloid Interface Sci.*, 68, 173 (1979).

Ramabhadran, T. E., T. W. Peterson, and J. H. Seinfeld, "Dynamics of Aerosol Coagulation and Condensation," *AIChE J.*, 22, 840 (1976).

Manuscript received October 1, 1979; revision received February 13, and accepted February 29, 1980.

Adsorption of Methane and Several Mixtures of Methane and Carbon Dioxide at Elevated Pressures and Near Ambient Temperatures on 5A and 13X Molecular Sieves by Tracer Perturbation Chromatography

The principles of tracer perturbation chromatography were applied to measure the sorption of pure methane and several methane-carbon dioxide mixtures on 5A and 13X molecular sieves at near ambient temperatures to pressures in excess of 7 MPa (1 000 lb/in.^{2}abs). The molecular sieves studied were industrial grade zeolite crystals pelleted with 20 wt % clay binder.

The statistical mechanical model of Ruthven was applied to both pure methane and to several mixtures of methane rich, methane-carbon dioxide mixtures from a few MPa (50 lb/in.^{2}abs) to pressures as high as 10.34 MPa (1 500 lb/in.^{2}abs) at near ambient temperature. While the theory appears to correlate the data well even at high pressures, some limitations of the theory begin to appear for the mixtures of higher dioxide concentrations.

PAUL D. ROLNIAK
and
RIKI KOBAYASHI

Department of Chemical Engineering
Rice University
P. O. Box 1892
Houston, Texas 77001

SCOPE

The extent, range or scope of the foregoing work covers the competitive adsorption of binary mixtures of dissimilar gases at elevated pressures. Although industrial adsorptive processes usually take place at elevated pressures involving mixtures, high pressure adsorption data of gases on molecular sieves have seldom been reported (Lederman and Williams, 1964). Choosing tracer perturbation chromatography as the technique, Gilmer and Kobayashi (1965) measured the adsorption of methane and several mixtures of methane and carbon dioxide up to 7 MPA (1 000 lb/in.^{2}abs.). Data are taken to allow a clear distinction to be made between Gibbs and absolute adsorption. The study includes the prediction of pure component and mixture adsorption K values by the Ruthven model (1971, 1975, 1976) for methane and carbon dioxide over the range of pressure covered in this work.

Paul D. Rolniak is with The Pace Company Consultants & Engrs., Inc., Rocky Mountain Division, Cherry Creek Plaza III, 650 S. Cherry St., Suite 400, Denver, Colorado 80222.